Published in final edited form as:
Dev Biol. 2007 August 1; 308(1): 144–157.

mef2ca is required in cranial neural crest to effect Endothelin1 signaling in zebrafish

Craig T. Miller[1,2,*,‡], **Mary E. Swartz**[1,*], **Patricia A. Khuu**[1,3], **Macie B. Walker**[1,4], **Johann K. Eberhart**[1], and **Charles B. Kimmel**[1]

1*Institute of Neuroscience, 1254 University of Oregon, Eugene, OR 97403, USA*

Abstract

Mef2 genes encode highly conserved transcription factors involved in somitic and cardiac mesoderm development in diverse bilaterians. Vertebrates have multiple *mef2* genes. In mice, *mef2c* is required for heart and vascular development. We show that a zebrafish *mef2c* gene (*mef2ca*) is required in cranial neural crest (CNC) for proper head skeletal patterning. *mef2ca* mutants have head skeletal phenotypes resembling those seen upon partial loss-of-function of *endothelin1 (edn1*). Furthermore, *mef2ca* interacts genetically with *edn1*, arguing that *mef2ca* functions within the *edn1* pathway. *mef2ca* is expressed in CNC and this expression does not require *edn1* signaling. Mosaic analyses reveal that *mef2ca* is required in CNC for pharyngeal skeletal morphogenesis. Proper expression of many *edn1*-dependent target genes including *hand2*, *bapx1*, and *gsc*, depends upon *mef2ca* function. *mef2ca* plays a critical role in establishing the proper nested expression patterns of *dlx* genes. *dlx5a* and *dlx6a*, known Edn1 targets, are downregulated in *mef2ca* mutant pharyngeal arch CNC. Surprisingly, *dlx4b* and *dlx3b* are oppositely affected in *mef2ca* mutants. *dlx4b* expression is abolished while the *edn1*-dependent expression of *dlx3b* is ectopically expressed in more dorsal CNC. Together our results support a model in which CNC cells require *mef2ca* downstream of *edn1* signaling for proper craniofacial development.

Keywords

mef2c; *edn1*; neural crest; pharyngeal skeleton; pharyngeal arch; *dlx*; *hand2*; zebrafish

Introduction

Mef2 (*myocyte enhancing factor*) genes encode MADS domain-containing transcription factors that play critical roles in mesoderm development in invertebrates and vertebrates (reviewed in Black and Olson, 1998). Mammals have four *mef2* genes (*mef2a*, *mef2b*, *mef2c*, and *mef2d*). Mice lacking *mef2c* function die during early embryonic development due to severe heart and vascular defects (Bi et al., 1999; Lin et al., 1998; Lin et al., 1997). In addition to cardiac and vascular expression domains, *mef2c* is expressed in postmigratory cranial neural crest (CNC) within pharyngeal arch primordia (Dodou et al., 2004; Edmondson et al., 1994).

[2]Present address: Department of Developmental Biology, 279 Campus Drive, Beckman Center B300, Stanford University School of Medicine, Stanford, CA 94305, USA
[3]Present address: Department of Biochemistry, Oregon State University, Corvallis, OR, 97331, USA
[4]Present address: Stowers Institute for Medical Research, 1000 E. 50th Street, Kansas City, MO 64110, USA
*these authors contributed equally
‡Correspondence author. E-mail address: ctm@stanford.edu Phone: 1-650-725-7599 Fax: 1-650-725-7739

The early embryonic lethality has, to date, precluded functional analysis in later *mef2c* expression domains such as CNC.

Most of the cartilages and bones of the vertebrate head are derived from CNC cells. In vertebrate embryos, three bilateral streams of CNC populate the first (mandibular), second (hyoid) and the set of more posterior branchial arches, respectively. Within each pharyngeal arch in gnathostome embryos, prominent dorsal and ventral cartilages form, separated by a dorsal-ventral joint. For example, in the first arch, CNC cells form an upper (dorsal) and lower (ventral) jaw, articulating at the jaw joint. One potential function of the *mef2c* CNC expression domain could be to regulate aspects of pharyngeal skeletal development. A critical signaling pathway that patterns CNC at the stages that *mef2c* has been reported to be expressed is Endothelin1 (Edn1),

Development of the lower jaw in mice, chicks, and fish requires Endothelin signaling (Clouthier et al., 1998; Kempf et al., 1998; Kurihara et al., 1994; Miller et al., 2000; Nair et al., 2007). Edn1, a secreted signaling molecule, is expressed in pharyngeal arch epithelia and mesoderm, and signals to CNC cells, which express the G-protein-coupled transmembrane Endothelin receptor *EdnrA* (reviewed in Clouthier and Schilling, 2004). Genetic work in mice and zebrafish have revealed other molecules involved in regulating or transducing the Edn1 signal during craniofacial development. In mice, mutation of *Edn1*, *EdnrA*, or an endothelin converting enzyme (*ECE1)* gives similar lethal craniofacial phenotypes where the lower jaw is hypoplastic and malformed (Clouthier et al., 1998; Kurihara et al., 1994; Yanagisawa et al., 1998). The proprotein convertase Furin has been shown to biochemically cleave Edn1, and in zebrafish, reducing *furin* function causes phenotypes resembling *edn1* mutants (Denault et al., 1995; Walker et al., 2006a). These studies suggest that Edn1 is cleaved twice, first by Furin and second by ECE1 and that these cleavages are required for Edn1 bioactivity. Further upstream of Edn1, the transcription factor Tbx1 is required in zebrafish for *edn1* pharyngeal arch expression (Piotrowski et al., 2003). In humans, mutation of *Tbx1* can cause one of the most common craniofacial defects, DiGeorge syndrome, highlighting the clinical importance of Edn1 signaling in craniofacial development (Jerome and Papaioannou, 2001; Lindsay et al., 2001; Merscher et al., 2001).

Downstream of EdnrA, G-proteins transduce the Edn1 signal, as mice doubly mutant for *GalphaQ* and *Galpha11* have *Edn1*-like craniofacial defects (Ivey et al., 2003). G-protein activation by EdnrA likely leads to activation of Phospholipase C (Plc), because in zebrafish, mutation of *plcβ3* causes phenotypes similar to *edn1* mutants and *plcβ3* and *edn1* interact genetically (Walker et al., 2006b). The Edn1 signal eventually activates a transcriptional hierarchy in CNC involving *Dlx5*, *Dlx6*, and *Hand2*(*dHAND*), and nearly all CNC expression of these three genes requires Edn1 signaling (Miller et al., 2003; Ruest et al., 2004; Walker et al., 2006a). *Dlx5* and *Dlx6* regulate the CNC expression of *Hand2 (dHAND)*, an effector of *edn1* signaling in mice and zebrafish (Charite et al., 2001; Depew et al., 2002; Miller et al., 2003; Ruest et al., 2004; Thomas et al., 1998). A *Hand2* pharyngeal arch enhancer requires *Edn1* signaling, as enhancer expression is absent in the arches of *EdnrA* mutant mice (Charite et al., 2001). Targeted deletion of this *Edn1*-responsive *Hand2* enhancer reveals it to be required for craniofacial development (Yanagisawa et al., 2003). Biochemical analyses of this *Hand2* pharyngeal arch enhancer found that this enhancer binds Dlx6 (but not Dlx2, Dlx3, or Dlx5) (Charite et al., 2001). Thus in mice, Dlx6 appears to participate in transducing the Edn1 signal to *Hand2*.

Dlx genes have nested expression patterns within each pharyngeal arch in mice, many aspects of which are conserved in zebrafish (Depew et al., 2002; Walker et al., 2006a). *Dlx1* and *Dlx2* are expressed broadly throughout seemingly all postmigratory pharyngeal arch CNC. *Dlx5* and *Dlx6* are more ventrally restricted within the pharyngeal arch primordia. *Dlx3* and

Dlx4 are even more ventrally restricted. Genetic experiments in the mouse have revealed this *Dlx* code to be of paramount importance in establishing regional identity within each pharyngeal arch (Depew et al., 1999; Depew et al., 2002; Depew et al., 2005; Qiu et al., 1995). *Dlx6*, together with *Dlx5*, specifies ventral identity within the pharyngeal arches. Mice doubly mutant for *Dlx5* and *Dlx6* have a fantastic homeotic phenotype in which the lower jaw is transformed into an upper jaw (Depew et al., 2002).

A similar ventral-to-dorsal transformation is seen in *Edn1* and *EdnrA* mutants (Ozeki et al., 2004; Ruest et al., 2004). In zebrafish mutant for Edn1 pathway genes or with reduced levels of Edn1, a ventral hyoid bone can be homeotically transformed into a more dorsal bone (Kimmel et al., 2003). Gene expression studies show that the dorsally restricted *eng2* expression ectopically expands ventrally in *edn1* mutants (Miller et al., 2003). Furthermore, overexpression of Edn1 protein can cause the reciprocal transformation, where dorsal cartilages appear transformed into ventral cartilages (Kimmel et al., 2007). Thus, *Edn1* is a master regulator of lower jaw and other ventral pharyngeal arch fates and in its absence the ventral arch assumes dorsal fates. *Edn1* seems to exert this regulation primarily through *Dlx* genes. Despite this fundamental importance of the *Dlx* genes, little is known about what establishes their nested expression patterns.

Large scale genetic screens in the zebrafish have identified over 100 loci required for head skeletal patterning (Neuhauss et al., 1996; Nissen et al., 2003; Piotrowski et al., 1996; Schilling et al., 1996). One class of mutations was put into an “anterior arch” class for phenotypically similar defects in the anterior pharyngeal arch skeleton, particularly the first and second arches. This anterior arch class contains four loci, *sucker*, *schmerle*, *sturgeon*, and *hoover* (Piotrowski et al., 1996). We've previously shown these first three loci to encode Endothelin1, FurinA, and Plcβ3, respectively (Miller et al., 2000; Walker et al., 2006a; Walker et al., 2006b).

Within this “anterior arch” class, both strong and weak phenotypes are seen. Strong phenotypes, represented by typical *edn1* and *plcβ3* mutants, include highly penetrant severe reduction of lower jaw and other ventral pharyngeal cartilages, absence of the jaw joint and other dorsal-ventral pharyngeal joints, and loss of ventral pharyngeal bones (Kimmel et al., 1998; Kimmel et al., 2003; Miller et al., 2000; Walker et al., 2006b). Weak phenotypes, represented by typical mutants for *furinA* and *hoover* mutants, or partial reduction of Edn1 signaling by morpholino knockdown, include only mild, if any, reductions in ventral cartilage, and incompletely penetrant absence of joints and expansion of hyoid pharyngeal bones (Kimmel et al., 1998; Kimmel et al., 2003; Miller and Kimmel, 2001; Walker et al., 2006a).

Here we present fine mapping, sequencing, and morpholino phenocopy data showing that *hoover* is the zebrafish *mef2ca* gene. *mef2ca* mutants have skeletal phenotypes resembling those seen upon partial reduction of *edn1* function. In addition to these striking phenotypic similarities, we find strong genetic interactions between *mef2ca* and *edn1* including dominant enhancement and an unpredicted partial rescue of the *edn1* phenotype in the double homozygote. *mef2ca* is expressed transiently in early postmigratory pharyngeal arch CNC. Mosaic analyses reveal *mef2ca* to function autonomously in CNC for pharyngeal skeletal patterning. *mef2ca* mutants exhibit similar, but less severe, gene expression defects as *edn1* mutants, such as reduced pharyngeal arch expression of *hand2*, *bapx1*, *gsc*, *dlx5a*, and *dlx6a*. Unexpectedly, we find opposite effects of *mef2ca* on the adjacent and convergently transcribed *dlx* gene pair *dlx3b* and *dlx4b*. *dlx4b* expression, normally restricted to the ventral most CNC, is almost completely lost in *mef2ca* mutants. In stark contrast, the *edn1*-dependent ventrally-restricted *dlx3b* expression expands dorsally in *mef2ca* mutants. Together our results reveal a role for *mef2c* in effecting the response to the Edn1 signal within CNC cells.

Methods

Fish maintenance and gynogenetic screens

Fish were raised and staged as described (Westerfield, 1993; Kimmel et al., 1995). *mef2ca (hoover)^{tn213}* mutant fish were generously provided by Drs. Tatjana Piotrowski and Christiane Nusslein-Volhard. *mef2ca^{b631}* and *mef2ca^{b1086}* were identified by screening ENU mutagenized gynogenetic clutches stained for head cartilage in fixed larvae and live Alizarin red staining, respectively (Kimmel et al., 2003; Miller et al., 2004). For phenotypic analyses, the strongest allele (see Table 1), *mef2ca^{b1086}* was used unless noted otherwise. *fli1*:*GFP* albino transgenic fish have been previously described (Lawson and Weinstein, 2002).

Mapping

For mapping, the *b631* mutation, which arose on an AB background, was crossed onto the *wik* mapping strain (Knapik et al., 1998). *b631/wik* heterozygotes were incrossed, generating clutches of mutant fish. At 4.5 days postfertilization (dpf), fish were anesthetized with MS222, then scored for facial phenotypes. A subset of each cross, including all fish with any facial aspects of the *b631* phenotype, was then euthanized with MS222 and bisected. The heads were arrayed on one set of 96-well plates, and the tails were arrayed on another. DNA was isolated from the tails while the heads were stained with Alcian green to visualize cartilage. Each stained head was then inspected under a dissecting scope for the characteristic aspects of the mutant phenotype (loss of dorsal/ventral pharyngeal joints, ectopic nodules of cartilage around the basihyal and/or ectopic medial processes extending from the palatoquadrate). This process identified over 1000 fish with the characteristic *b631* cartilage phenotypes, which we used as our mapping panel. Of these, 504 fish were polymorphic and succesfully genotyped for all of the markers shown in Fig. 1A. To map *mef2ca*, a polymorphism in the 3′UTR was revealed by PCR amplification with primers ATGTCCTGAACAATGCTAAG and CACATCCGCTCGTAATTGAGT and cutting with RsaI. Marker z9701 was amplified using primers GTGTGTGCTGCAAGAGTTCAG and ATGTAAAACGCTGGTGTTTGTG.

Sequencing

We sequenced *mef2ca* from wild-type and mutant genomic DNA by amplifying the previously reported exons by RT-PCR or with primers designed to flanking intronic sequences designed from the zebrafish genome assembly (http://www.ensembl.org/Danio_rerio/index.html). We note that the *mef2ca* sequence we obtained from both the AB and tlf backgrounds differs from the published sequence (Ticho et al., 1996, Genbank accession #U66569) at amino acid position 163, with their sequence having an ATG or methionine codon, and all of our sequences having a CTG or leucine codon.

Morpholino injections

For morpholino injections, a *mef2ca* morpholino oligonucleotide (MO) (TTCCTTCCTCTTCCAAAAGTACAGT), and an *edn1* MO (GTAGTATGCAAGTCCCGTATTCCAG) were injected as described, (Miller and Kimmel, 2001). Roughly 5 nL was pressure-injected into the yolks of 1-4 cell embryos. Surviving larvae at day 4 were Alcian stained and scored for head skeletal phenotypes.

Tissue labeling procedures.

Alcian Green was used to stain the cartilage of fixed larvae as described (Miller et al., 2003). Facial cartilages were dissected out and prepared as flat mounts (Kimmel et al., 1998). Double Alcian Blue (cartilage) and Alizarin Red (bone) staining was done on fixed larvae using a modified “acid-free” protocol (Walker and Kimmel, in press). Wholemount RNA in situ hybridizations were performed as described (Miller et al., 2000) using previously described

probes: *mef2ca* (Ticho et al., 1996), *hand2* (Angelo et al., 2000), *bapx1* (Miller et al., 2003), *goosecoid* (Schulte-Merker et al., 1994), *dlx2a* and *dlx3b* (Akimenko et al., 1994), *dlx4b* (Liu et al., 2003), and *dlx5a* and *dlx6a* (Walker et al., 2006a).

For in situ hybridization, embryos were raised in 0.0015% PTU (1-phenyl 2-thiourea) to inhibit melanogenesis (Westerfield, 1993). The lesion in *mef2ca*^{b1086} mutants was genotyped by PCR amplification with primers TGCGGCTCGTTGTACTCGAAGTATT and TCATCAGGTTACGTTTACAAAGAGGAAGTTT, followed by digestion XmnI. See (Neff et al., 1998) for dCAPS genotyping method. *edn1*^{tf216b} mutants were PCR genotyped as described (Miller et al., 2000).

Mosaic analyses

Neural crest cell transplants were performed between wild-type and *mef2ca*^{b1086} embryos in a *Tg(fli1:egfp)*^{y1} background as previously described (Crump et al., 2004). Labeled cells were taken from donor embryos and placed 90 degrees from dorsal in host embryos at shield stage. Embryos were imaged at 30 hpf and re-imaged at 5dpf, followed by cartilage and bone double staining and flat mounting for imaging.

Results

Molecular identification of lesions in zebrafish mef2ca

By screening mutagenized gynogenetic diploid clutches for larval head skeletal phenotypes, we identified two new mutations, *b631* and *b1086*, which both cause phenotypes similar to those seen upon mutation of the locus *hoover* (see below). A single allele of *hoover*, *tn213*, was previously identified in a large scale mutagenesis screen (Piotrowski et al., 1996). Complementation analyses revealed that *b631*, *tn213* and *b1086* are all allelic (data not shown).

Using bulked segregant analyses, we genetically mapped *b631* to distal LG10 closely linked to microsatellite z9701. We refined the map position to 0.36 cM distal to z21976 and 0.1 cM proximal to z9701 (Fig. 1A). A previously published zebrafish *mef2c* gene had been mapped close to z9701 (Kelly et al., 2000;Ticho et al., 1996). We refer to this gene as *mef2ca*, as we subsequently identified an unlinked duplicate zebrafish *mef2c* gene, *mef2cb* (M.B. W., unpublished data). We mapped *mef2ca* to the same interval as *hoover*, non-recombinant in 1008 meioses (Fig. 1A). Thus, *mef2ca* is an outstanding positional candidate for *hoover*.

Sequencing *mef2ca* in all three *hoover* mutant alleles revealed lesions predicted to result in loss-of-function alleles (Fig. 1B). An A-to-T transversion at nucleotide 172 introduces a predicted early stop codon upstream of the MEF2 domain in *b1086* mutants. In *tn213* mutants, A T-to-C transition at the second nucleotide of the intron seven splice donor results in a predicted transcript that would be aberrantly spliced. In *b631* mutants, an A-to-C transversion changes the start methionine codon to a leucine codon. Together, these mapping and sequencing data strongly indicate that *hoover* is zebrafish *mef2ca*, and we hereafter refer to this locus as *mef2ca* for clarity and simplicity.

Mutation of mef2ca causes phenotypes resembling partial reduction-of-function of Edn1 phenotypes

All three *mef2ca* mutant alleles are characterized by larval craniofacial phenotypes resembling partial reduction of function of *edn1* (Fig. 2; Table 1) (Kimmel et al., 2003;Miller and Kimmel, 2001;Piotrowski et al., 1996;Walker et al., 2006a). The mouth is displaced ventrally, and joints between dorsal and ventral cartilages in the anterior pharyngeal arches are lost (Fig. 2,Table 1). Ectopic cartilage nodules are typically seen located around the second arch midline cartilage, the basihyal. Ectopic cartilage processes are typically seen emanating medially off

of the first arch upper jaw cartilage, the palatoquadrate (Fig. 2,Table 1). The dorsal and ventral hyoid bones, the opercle and branchiostegal ray, are expanded and often fused to each other, often causing the ventral branchiostegal ray to appear homeotically transformed into an opercle (Fig. 2C,D and see Kimmel et al., 2003). Phenotypically, the three alleles form an allelic series, with *b1086* being the most severe, and *b631* being the least severe (Table 1). Reducing *mef2ca* function with morpholino oligonucleotides (MOs) robustly phenocopies multiple aspects of the *mef2ca* phenotype in a dose-dependent fashion (Fig. 2E-F, Table 1). These *mef2ca* mutant and mef2ca-MO-injected cartilage phenotypes strikingly resemble the phenotypes seen upon partial reduction of *edn1* or strong reduction in *furinA* function (see Intro). Injecting low doses of edn1-MOs spares ventral cartilage formation but abolishes joint formation and results in cartilage nodules and processes similar to those seen in *mef2ca* mutants (Table 1, Fig. 2G-I).

mef2ca interacts genetically with edn1

Our analyses of the facial skeletal phenotype show that strong loss of function of *mef2ca* produces phenotypes resembling partial reduction of *edn1* function or reductions of Edn1-pathway genes described in the Introduction. The resemblances include the losses of the DV joints, the enlarged opercular-branchiostegal dermal bones, and weak reductions of the ventral cartilages. To learn if these similarities are because the genes function in a common genetic pathway, we analyzed skeletal phenotypes of *mef2ca; edn1* double mutants. We observe prominent epistasis that allow ordering the two genes in a hierarchical pathway.

Surprisingly, reduction or loss of *mef2ca* function results in partial rescue of the $edn1^{-/-}$ skeletal phenotypes. We illustrate with individual cases (Fig. 3), before coming to quantitative analyses (Fig. 4). We focus on the hyoid arch for these analyses: The $edn1^{-/-}$ homozygous single mutant shows invariable loss of the joint between dorsal (HS) and ventral (CH) cartilage, and invariable severe reduction in the size of CH. Sometimes, the CH can appear to be missing altogether (Fig. 3G, especially on one side of this mutant). The hyoid dermal bone is often severely reduced as well (Fig. 3G, especially on the other side in this instance). The double mutant shows the joint loss, and in comparison with $edn1^{-/-}$ single mutant shows a larger CH (Fig. 3I, arrowhead) and expanded dermal bone (the OP), i.e., more like the $mef2ca^{-/-}$ single mutant (Fig. 3C) and the wild-type condition (Fig. 3A).

In contrast to this rescue (or suppression) of the $edn1^{-/-}$ phenotype, we see a striking enhancement of the phenotype of the $edn1^{+/-}$ heterozygote with loss of a single wild-type allele of *mef2ca* (i.e., in the double heterozygote, $edn1^{+/-}$; $mef2ca^{+/-}$, Fig. 3E). In the example shown dermal bone is dramatically enlarged, and the DV joint is lost (*) on one side of the fish, whereas the phenotype on the other side of this animal appears wild type, the usual case for the single heterozygote, $edn1^{+/-}$; $mef2ca^{+/+}$.

To examine these interactions quantitatively, we scored both the dermal bone (OP) and cartilage (CH) phenotypes according to severity in fish from all nine possible genotypic combinations of *mef2ca* and *edn1* mutant alleles (shown in Fig. 3). For the bone we see a mild *edn1* loss-of-function phenotype in the $mef2ca^{-/-}$; $edn1^{-/-}$ double homozygous mutant, and no effect of adding 1 or 2 $edn1^{+}$ alleles in the absence of any $mef2ca^{+}$ alleles (Fig. 4A). In contrast, adding $mef2ca^{+}$ alleles in the absence of $edn1^{+}$ alleles yields more severe bone phenotypes in a dose-dependent manner (Fig. 4B). The straight-forward interpretation is that *mef2ca* is acting as a repressor. The function of *edn1* in dermal bone development becomes clear when wild-type alleles of the two genes are combined (Fig. 4C); even only a single $edn1^{+}$ allele strongly reverses the *mef2ca* repression. Hence *edn1* acts hierarchically upstream of *mef2ca*, serving to repress the repressor (Fig. 4G).

Similar analysis of the CH phenotype shows a variation on this theme. Whereas *mef2ca* again shows itself to be repressing skeletal development (Fig. 4E) and *edn1* again reverses this repression (Fig. 4F), a separate, additional function of Edn1 is apparent when examined in the *mef2ca*$^{-/-}$ background (Fig. 4E), namely a *mef2ca*-independent activation of CH development (Fig. 4D). Hence, whereas *edn1* may be regulating dermal bone entirely through repressing *mef2ca*, it regulates ventral cartilage size in both a *mef2ca*-dependent and *mef2ca*-independent fashion (Fig. 4G).

mef2ca is expressed in early postmigratory pharyngeal arch CNC and later in pharyngeal arch muscle cores

If, as our epistasis evidence suggests, Mef2ca functions downstream of Edn1, then we predict *mef2ca* to be expressed in CNC-derived arch mesenchyme, the target of Edn1 signaling. In the mouse, *mef2c* expression during embryonic development is detected in complex and dynamic patterns in CNC, cardiac and skeletal muscle, the vasculature, and the CNS (De Val et al., 2004; Dodou et al., 2004; Edmondson et al., 1994; Lyons et al., 1995). Consistent with the mouse expression pattern, we find transient expression of *mef2ca* in pharyngeal arch CNC. At 20 hpf, we detect *mef2ca* expression in mandibular, hyoid and branchial CNC (Fig. 5A,B). This CNC expression domain does not appear to require *edn1* signaling, as expression appears unchanged in *edn1* mutants (Fig. 5C). Reciprocally, the expression of *edn1* in arch epithelia and mesodermal cores appears unaffected in *mef2ca* mutants (data not shown). *mef2ca* CNC expression is dynamic and seems to sweep in an anterior-posterior fashion in that expression at 24 hpf is strongest in the third arch, at 30 hpf is strongest in the fourth arch, and at 32 hpf is strongest in the fifth arch (data not shown).

Beginning around 30 hpf, we detect *mef2ca* expression in pharyngeal arch muscle cores, first appearing in the adductor mandibulae core in the first arch (data not shown). By 55 hpf, all cranial muscle cores and differentiating head muscles express *mef2ca* (Fig. 5D). While the *mef2ca* head mesoderm expression is detectable after stages known to be critical for transmission of the Edn1 signal, the CNC expression domain is in precisely the right place and at the right time to transduce the Edn1 signal (Miller et al., 2000).

mef2ca is autonomously required in cranial neural crest

If *mef2ca* functions downstream of *edn1* in CNC, *mef2ca* should function autonomously in CNC to regulate head skeletal development, a hypothesis we can directly test by mosaic analysis. We transplanted wild-type CNC unilaterally into *mef2ca* mutant hosts (Fig. 6A,B). We found that wild-type CNC can rescue skeletal patterning on the transplanted side, while the non-transplanted control side exhibits the characteristic *mef2ca* mutant phenotypes (Fig. 6C). In every instance (n=7), wild-type CNC cells rescued the cartilage morphology of mutant hosts on the transplanted side. In contrast, the control side exhibited the mutant phenotype 100% of the time. Additionally, in reciprocal transplants, *mef2ca* mutant CNC conferred a mutant cartilage phenotype in 88% (n=7/8) of experimental sides . Thus *mef2ca* functions autonomously in CNC for pharyngeal cartilage morphogenesis. Together our epistasis and mosaic analyses indicate that *mef2ca* functions as a downstream effector of *edn1* in CNC cells.

mef2ca is required for expression of *edn1*-dependent genes

We next asked where *mef2ca* functions in the cascade of known effectors of *edn1* signaling in CNC. We previously identified two transcription factors that partially mediate the *edn1*-dependent processes of ventral cartilage and joint formation. The bHLH transcription factor Hand2, whose ventrally-restricted expression is dramatically reduced in *edn1* mutants, is also required for ventral pharyngeal cartilage formation (Miller et al., 2003). Hand2 is also known to physically interact with Mef2c (Zang et al., 2004). A second effector of Edn1 signaling is the homeobox transcription factor Bapx1, which is required for jaw joint formation in the

mandibular arch (Miller et al., 2003). *bapx1* is expressed in an intermediate first arch expression domain in wild types, but this domain is absent in *edn1* mutants. As *mef2ca* mutants typically lack jaw joints, and variably have ventral cartilage reduction, we asked whether *mef2ca* functions upstream of these two *edn1* effectors by examining the expression of *hand2* and *bapx1* in *mef2ca* mutants. At 30 hpf, the ventral arch expression of *hand2* is downregulated in *mef2ca* mutants (Fig. 7A,B). However, by 55 hpf, ventral arch *hand2* expression has recovered in *mef2ca* mutants (Fig. 7C-F), similar to *furinA* mutants, but unlike *edn1* mutants (Walker et al., 2006a). At 48 hpf, the intermediate first arch domain of *bapx1* is downregulated in *mef2ca* mutants (Fig. 7G,H).

In the second (hyoid) arch of wild types, *gsc* is expressed in dorsal and ventral domains, but not in the intermediate domain, which includes the presumptive joint (Crump et al., 2006; Miller et al., 2000; Walker et al., 2006a). In *edn1* mutant zebrafish, ventral arch two expression of *goosecoid* (*gsc*) is missing, while dorsal arch two *gsc* expression ectopically expands into the intermediate domain (Miller et al., 2000; Walker et al., 2006a; Walker et al., 2006b). Like *edn1* mutants, *mef2ca* mutants have reduced ventral arch two expression of *gsc*. However, unlike *edn1* mutants, and also unlike *plcβ3* and *furinA* mutants, *mef2ca* mutants have no detectable ectopic expression of *gsc* in the intermediate hyoid domain (Fig. 7I,J). Thus, consistent with the phenotypic similarities of *mef2ca* and *edn1* mutants, we find *mef2ca* also regulates these three *edn1*-dependent genes. Paralleling the less severe skeletal phenotype of *mef2ca* mutants, expression of *hand2*, *bapx1*, and *gsc* are affected less severely in *mef2ca* mutants than in *edn1* mutants.

mef2ca activates *dlx5a*, *dlx6a*, and *dlx4b*, but represses *dlx3b*

Critical homeotic effectors of *edn1* signaling are *dlx* genes, which in mice function at least in part upstream of *hand2* (Depew et al., 2002; Ozeki et al., 2004; Ruest et al., 2004). We previously showed that in *edn1* mutants, the ventrally-restricted pharyngeal arch CNC expression of *dlx5a*, *dlx6a* and *dlx3b* are extremely reduced, while the widespread expression of *dlx2a* was only effected in the ventral-most CNC (Miller et al., 2000; Walker et al., 2006a). Furthermore, we showed that reduction of *dlx3b* and *dlx5a* function causes phenotypes similar to the *mef2ca* mutant phenotype (Walker et al., 2006a). Given these functions and *edn1*-dependent expression domains of *dlx* genes, we tested the hypothesis that *mef2ca* functions as an upstream activator of *dlx* genes by assaying *dlx* expression in arch primordia of *mef2ca* mutants. Like in *edn1* mutants, the broad CNC expression of *dlx2a* appears largely unaffected in *mef2ca* mutants (Fig. 8A,B). As expected and like *hand2* and *bapx1*, *dlx5a* and *dlx6a* are downstream of *mef2ca*, as pharyngeal arch CNC expression of both genes is downregulated in *mef2ca* mutants (Fig. 8C-F). Contrary to our prediction, the *edn1*- dependent ventrally-restricted *dlx3b* expression expands dorsally in *mef2ca* mutants (Fig. 8G,H). Thus, *mef2ca* does function upstream of *dlx3b*, but represses *dlx3b* expression in more intermediate domains. Conversely, expression of the convergently transcribed linked *dlx* gene, *dlx4b*, is severely downregulated in *mef2ca* mutants (Fig. 8I,J). Thus, *mef2ca* plays a crucial role in effecting the Edn1 signal to establish the correctly nested expression patterns of *dlx* genes.

Discussion

We present fine mapping, sequencing, and morpholino phenocopy results that together reveal a critical role for *mef2ca* in patterning the pharyngeal skeleton. The skeletal and gene expression similarities of *mef2ca* mutants and animals with reduced *edn1* function support a model in which *mef2ca* functions in the same pathway as *edn1*. Epistasis analyses order *mef2ca* function downstream of *edn1*. Our expression and mosaic analyses support this model, and demonstrate *mef2ca* to be required in CNC, the tissue which receives the Edn1 signal from the surrounding epithelial and mesodermal environment. While *mef2ca* expression in CNC

does not require Edn1 signaling, *mef2ca* is required for aspects of the *edn1*-dependent activation of *hand2*, *bapx1*, *gsc*, *dlx5a*, *dlx6a*, and *dlx4b*, and represses *edn1*-dependent *dlx3b* expression.

A zebrafish mef2c gene is required in CNC for Edn1 signal transduction

In mice, *Mef2c* plays critical roles in patterning mesodermal tissue in the heart and vasculature. Mice deficient for *Mef2c* die around e9.5, lacking a right ventricle and displaying complex vascular defects (Bi et al., 1999; Lin et al., 1998; Lin et al., 1997). While cardiac and vasculature expression domains of *Mef2c* likely underlie these early phenotypes, *Mef2c* is expressed in many other domains (Dodou et al., 2004; Edmondson et al., 1994). For example, in the embryonic pharyngeal arches, *Mef2c* is expressed in postmigratory CNC (Dodou et al., 2004).

Here we show a critical role for a zebrafish *mef2c* gene, *mef2ca*, in patterning the CNC-derived head skeleton. *mef2ca* mutant zebrafish have pharyngeal skeletal defects resembling defects seen upon partial reduction of *edn1* function. The more mild skeletal phenotypes seen in *mef2ca* mutants compared to *edn1* mutants might be explained by the fact that there are other *mef2* genes in zebrafish, any one or more of which could act redundantly with *mef2ca* in the CNC. If so, the condition would be similar to *furin* genes (Walker et al., 2006a), where duplicate copies in fish allow roles in later developmental processes to be uncovered and studied.

Similarly, the less severe phenotype of zebrafish *mef2ca* mutants compared to the early embryonic lethality of mouse *mef2c* mutants could be explained in part by redundant roles of *mef2ca* and a second *mef2c* gene in zebrafish, *mef2cb*. Consistent with this model, we detect expression of both *mef2ca* and *mef2cb* during heart development (M.E.S. and M.B.W., unpublished results). Future studies can test whether *mef2ca* and *mef2cb* are functionally redundant in zebrafish, as we predict.

The genetic alleles of *mef2ca* appear to represent an allelic series. The weakest *mef2ca* allele, *b631*, is clearly a hypomorphic allele, as it arose on and was maintained on the same inbred genetic background as *b1086*, but results in lower penetrance and expressivity. The phenotypically intermediate allele, *tn213*, arose on and has been maintained on a different genetic background as the other two alleles, which could account for some or all of the differences in it's penetrance and/or expressivity from the other two alleles. The phenotypically strongest *mef2ca* allele, *b1086*, is predicted to result in a protein lacking the MEF domain and carboxyl terminus, which are required for Mef2c function (Molkentin et al., 1996a). Furthermore expression of *mef2ca* in *b1086* mutants appears severely reduced by in situ hybridization (M.E.S., unpublished data). Thus, *b1086* is clearly at least a strong loss-of-function allele, and likely a null.

Together our phenotypic, epistasis, mosaic, and gene expression results indicate that *mef2ca* functions within CNC downstream of Edn1 signaling. Unlike other previously identified downstream targets of Edn1 signaling, transcription of *mef2ca* in CNC cells does not require Edn1 signaling. Thus, the requirement of *mef2ca* for *edn1*- dependent gene expression must be a mechanism other than a sequential transcriptional hierarchy. During myogenesis, class II histone deacetylases (HDACs) regulate MEF2 protein activity by binding to MEF2 and repressing MEF2's ability to transactivate (reviewed in McKinsey et al., 2001). Chang et al., (2005) showed that signaling from G-protein coupled receptors, including EdnrA, leads to phosphorylation of class II HDACs which has been shown to cause dissociation from MEF2 (Chang et al., 2005; Lu et al., 2000). Perhaps in CNC cells, activation of EdnrA by Edn1 signaling signals to Mef2ca through HDAC regulation. Alternatively, Edn1 signaling could effect Mef2c more directly and involve one or more of the known post-transcriptional modifications to Mef2 proteins, such as phosphorylation or sumoylation, or an effect on the

nuclear or subnuclear localization (De Angelis et al., 1998; Gregoire et al., 2006; Gregoire and Yang, 2005; Han et al., 1997; Kato et al., 2000; Lazaro et al., 2002; Molkentin et al., 1996b). Future research can determine how Mef2ca is activated in CNC by Edn1 signaling.

mef2a is required for proper expression patterns of dlx genes

The primacy of the master regulator Edn1 for lower jaw development has been demonstrated in the mouse. Both *Edn1* and *EdnrA* mutant mice display similar homeotic transformations as those first reported for the *Dlx5; Dlx6* double mutant mice (Depew et al., 2002; Ozeki et al., 2004; Ruest et al., 2004). These phenotypic similarites between Edn1 pathway mutants and *Dlx5; Dlx6* double mutants, together with the findings that in mice and fish CNC expression of *dlx5* and *dlx6* requires *edn1* signaling (Ruest et al., 2004; Walker et al., 2006a), identify Dlx transcription factors as critical effectors of the Edn1-mediated program of intermediate and ventral pharyngeal arch development. We find that CNC expression of both *dlx5a* and *dlx6a* also depends on *mef2ca*. Thus *mef2ca* functions in CNC to transduce the Edn1 signal to *dlx* genes.

The ventral to dorsal homeotic transformation seen in *Dlx5; Dlx6* mutant mice provides strong support for the model of a Dlx code where dorsal-ventral fates in pharyngeal arches are assigned according to the combination of *Dlx* genes expressed. Functional analysis of other *Dlx* genes supports this idea of a Dlx code (Depew et al., 1999; Depew et al., 2002; Depew et al., 2005; Qiu et al., 1995). Although mice homozygous for *Dlx3* mutations die during early embryonic development due to placental defects, precluding analysis of the head skeleton (Morasso et al., 1999), Depew et al. demonstrated a genetic interaction between *Dlx3* and *Dlx5*. *Dlx3* heterozygosity results in distinctive additional craniofacial phenotypes occuring on a $Dlx5^{-/-}$ mutant background (Depew et al., 2005). In zebrafish, *dlx3* and *dlx5* also interact, as reducing *dlx3b* and *dlx5a* function with morpholino oligonucleotides results in craniofacial phenotypes similar to *mef2ca* mutants (Walker et al., 2006a). It is interesting that in these same experiments, reduction of *dlx5a* and *dlx6a* did not produce dramatic ventral-to-dorsal homeotic transformations as seen in mice. This could either reflect incomplete knockdown of these genes by morpholinos, or reveal differences in *dlx* gene function between mice and fish. However, these experiments establish that *dlx3b* and *dlx5a* both participate in zebrafish craniofacial development.

Despite this fundamental importance of *dlx* genes in patterning the face, little is known about the molecular mechanisms that establish their nested expression patterns. Our finding that *mef2ca* mutants display ectopic intermediate domain expression of *dlx3b* suggests that the establishment of the nested *dlx* expression domains involves repression of ventrally-restricted *dlx* genes from more dorsal domains, with *mef2ca* mediating this dorsal repression of *dlx3b*. Thus, *mef2ca* plays multiple roles in establishing a Dlx code. In addition to being required for the expression of *dlx4b, dlx5a*, and *dlx6a* in intermediate and ventral domains, *mef2ca* restricts *dlx3b* expression from more dorsal domains. This dorsal repression of *dlx3b* was unpredicted, as *dlx3b* requires *edn1* signaling (Miller et al., 2000; Walker et al., 2006a). Although both *edn1* and *mef2ca* function upstream of *dlx3b*, they exert opposite regulatory influences. We propose that the *edn1* activation of *dlx3b* expression occurs through *mef2ca*-independent (see below).

Molecular genetic analyses of *dlx* cis-regulation have identified conserved enhancers driving pharyngeal arch expression. A conserved enhancer between *dlx3* and *dlx4* is both necessary and sufficient for pharyngeal arch expression in mice (Sumiyama et al., 2003). Another conserved enhancer between *dlx5* and *dlx6* is also sufficient to drive expression in arch CNC in mice, and is dependent upon *Edn* signaling (Ghanem et al., 2003; Park et al., 2004). Whether *mef2ca* directly regulates *dlx* expression and how *mef2ca* exerts opposite regulation of *dlx3b* and *dlx4b* are interesting questions for future research.

A genetic model for the Edn1 network of craniofacial development

Our identification of *mef2ca* as a critical effector of Edn1 signaling further elaborates a model of the genetic circuitry controlling craniofacial development in zebrafish. Upstream of *edn1* in arch epithelia and mesoderm, *tbx1* and *wdr68* positively regulate *edn1* expression (Nissen et al., 2003; Piotrowski et al., 1996). Furin cleaves Edn1, followed by ECE1 cleavage, to produce the biologically active mature Edn1 ligand (Denault et al., 1995; Walker et al., 2006a; Xu et al., 1994). The mature secreted Edn1 ligand binds to, and activates, EdnrA receptors, which are required for Edn1 signaling in both mice and fish (Clouthier et al., 1998; Nair et al., 2007). Next, G-protein activation by EdnrA would signal to Plc (Ivey et al., 2003; Walker et al., 2006a). Our mosaic and gene expression analyses of *mef2ca* mutants place *mef2ca* as the most upstream known transcription factor that transduces the Edn1 signal in zebrafish. *mef2ca* transcription in CNC cells is apparently unaltered in *edn1* mutants, thus we propose that some posttranscriptional alteration to Mef2ca occurs upon Edn1 signaling (e.g. dissociation of a MEF2/HDAC complex by HDAC phosphorylation upon EdnrA activation, see above and Chang et al., 2005). Mef2ca then either directly or indirectly transactivates the CNC expression of *dlx5a, dlx6a, hand2,* and *bapx1*. As *dlx5a, hand2,* and *bapx1* are all required in some context for proper joints and/or ventral pharyngeal cartilage development, the failure to properly express these downstream genes in *mef2ca* mutants likely partially underlies the *mef2ca* mutant head skeletal phenotypes (Miller et al., 2003; Walker et al., 2006a).

Our data suggests that additional *mef2ca*-independent pathways likely transduce other branches of the Edn1 signal. For instance, while Edn1 is required for most ventral arch early and late *hand2* expression and all jaw joint *bapx1* expression, *mef2ca* only contributes to early *hand2* expression and is only required for some *bapx1* expression. Furthermore, the expression of *dlx3b* is repressed by *mef2ca* but activated by *edn1*. The expression of *gsc* is also ectopically activated in the intermediate hyoid arch in *edn1* and *furinA* mutants, but not *mef2ca* mutants. We propose that other *mef2* genes play roles in at least some of these *mef2ca*-independent processes.

That *mef2ca* mutations partially rescue or suppress the *edn1* mutant bone and cartilage phenotypes provides strong evidence that *mef2a* and *edn1* interact genetically, which we also infer from the similar gene expression and skeletal phenotypes seen in the two single mutants. One potential explanation for these results, supported by our epistasis analyses, is that *mef2ca* represses skeletal development and that *edn1* represses *mef2ca* function (see Fig. 4G). Consistent with this model, emphasizing repression, all four of the typical *mef2ca* mutant phenotypes (joint loss, ectopic cartilage nodules, ectopic processes emanating off of the upper jaw cartilage, enlarged opercle bone) represent inappropriate overdevelopment of skeletal structures. However, at the level of target genes we see a positive, not negative, function in *mef2ca* regulation of the *edn1*-dependent transcription of *hand2*, a gene required for ventral cartilage development, and, as well, for correct patterning of some features of the intermediate domain. Thus, *mef2ca* is clearly not simply repressing the Edn1-dependent transcriptional cassette. *dlx3b* stands out as the only gene we have found to be repressed by *mef2ca*. We hypothesize that the repression of *dlx3b* contributes to the rescue of the *edn1* mutant phenotypes by *mef2ca* mutations.

We summarize our major findings, and put them in context of previous work, with a model (Fig. 9). Secreted from ventral arch epithelia and mesoderm, the secreted Edn1 forms a gradient, with high levels ventrally, and low levels dorsally. The Edn1 signal is received by early postmigratory CNC cells, which interpret the gradient to specify fates along the DV axis. *mef2ca* is broadly expressed in CNC and exerts opposite effects on downstream effectors. In part via *dlx* genes, which *mef2ca* itself regulates, *mef2ca* mediates transduction of the *edn1* signal to *bapx1* and *hand2* in intermediate and ventral cells.

The downregulation of *hand2* in *mef2ca* mutants argues that *mef2ca* functions upstream of *hand2* transcription in ventral CNC cells (Fig. 9). Since we find *dlx5a* and *dlx6a* to be downregulated in ventral CNC cells of *mef2ca* mutants, and *dlx5* and *dlx6* function upstream of *hand2* expression in ventral CNC in mice (Depew et al., 2002), we propose that the positive regulation of *hand2* by *mef2ca* occurs via *dlx* genes including *dlx5a* and *dlx6a*. The epistatic relationship of *mef2ca* and *hand2* can be tested by analyzing animals with mutant alleles for both *mef2ca* and *hand2*, as we have done here for *mef2ca* and *edn1*.

The interaction between *mef2ca* and *hand2* is of particular interest because of our previous findings that at the level of target gene regulation in the pharyngeal arch mesenchyme, *hand2* itself is prominently, or entirely, functioning as a repressor (Miller et al., 2003). Repression of ventrally expressed genes, such as the *edn1*-dependent *msxE* and *msxB*, was unexpected since *hand2* mutants, like *edn1* mutants, lack nearly all ventral cartilage. In a manner that we don't yet understand, repression of *hand2* target gene function must be transposed into activation of skeletal development by the same cells. Since *hand2* expression is only transiently downregulated in *mef2ca* mutants, it is likely that the important time of *hand2* function for ventral cartilage to be made is relatively late in the patterning and morphogenesis of pharyngeal arch mesenchyme. This finding is just as we showed previously for the function of furinA, and we presented a model that the intermediate domain and ventral domain are dynamically segregating during the critical period when hand2 must function (Walker et al. 2006a). Our new findings, especially the repression of *dlx3b* by *mef2ca* that we report in this paper, reveal the genetic circuitry of the downstream response to *edn1* in CNC to be intricate and show frequent repression. The identification of additional molecules involved in transducing the Edn1 signal, as forward genetics in zebrafish has allowed, provides key progress toward a molecular genetic understanding of how the face is patterned.

Acknowledgments

We thank Will Talbot and Heather Stickney for mapping the b1086 allele, current and former members of the Kimmel laboratory, particularly Gage Crump, Tom Schilling, and Bruce Draper for useful discussions and suggestions, UO zebrafish researchers for their contributions to the ENU mutagenesis screens, and John Dowd for fish husbandry. Research support was provided by NIH grants DE13834, HD22486, an NRSA to J.K.E., and NIH training grant GM07413.

References

Akimenko MA, et al. Combinatorial expression of three zebrafish genes related to distal-less: part of a homeobox gene code for the head. J Neurosci 1994;14:3475–86. [PubMed: 7911517]

Angelo S, et al. Conservation of sequence and expression of Xenopus and zebrafish dHAND during cardiac, branchial arch and lateral mesoderm development. Mech Dev 2000;95:231–7. [PubMed: 10906469]

Bi W, et al. The transcription factor MEF2C-null mouse exhibits complex vascular malformations and reduced cardiac expression of angiopoietin 1 and VEGF. Dev Biol 1999;211:255–67. [PubMed: 10395786]

Black BL, Olson EN. Transcriptional control of muscle development by myocyte enhancer factor-2 (MEF2) proteins. Annu Rev Cell Dev Biol 1998;14:167–96. [PubMed: 9891782]

Chang S, et al. An expression screen reveals modulators of class II histone deacetylase phosphorylation. Proc Natl Acad Sci U S A 2005;102:8120–5. [PubMed: 15923258]

Charite J, et al. Role of Dlx6 in regulation of an endothelin-1-dependent, dHAND branchial arch enhancer. Genes Dev 2001;15:3039–49. [PubMed: 11711438]

Clouthier DE, et al. Cranial and cardiac neural crest defects in endothelin-A receptor-deficient mice. Development 1998;125:813–24. [PubMed: 9449664]

Clouthier DE, Schilling TF. Understanding endothelin-1 function during craniofacial development in the mouse and zebrafish. Birth Defects Res C Embryo Today 2004;72:190–9. [PubMed: 15269892]

Crump JG, et al. Moz-dependent Hox expression controls segment-specific fate maps of skeletal precursors in the face. Development 2006;133:2661–9. [PubMed: 16774997]

Crump JG, et al. An integrin-dependent role of pouch endoderm in hyoid cartilage development. PLoS Biol 2004;2:E244. [PubMed: 15269787]

De Angelis L, et al. Inhibition of myogenesis by transforming growth factor beta is density-dependent and related to the translocation of transcription factor MEF2 to the cytoplasm. Proc Natl Acad Sci U S A 1998;95:12358–63. [PubMed: 9770491]

De Val S, et al. Mef2c is activated directly by Ets transcription factors through an evolutionarily conserved endothelial cell-specific enhancer. Dev Biol 2004;275:424–34. [PubMed: 15501228]

Denault JB, et al. Processing of proendothelin-1 by human furin convertase. FEBS Lett 1995;362:276–80. [PubMed: 7729512]

Depew MJ, et al. Dlx5 regulates regional development of the branchial arches and sensory capsules. Development 1999;126:3831–46. [PubMed: 10433912]

Depew MJ, et al. Specification of jaw subdivisions by Dlx genes. Science 2002;298:381–5. [PubMed: 12193642]

Depew MJ, et al. Reassessing the Dlx code: the genetic regulation of branchial arch skeletal pattern and development. J Anat 2005;207:501–61. [PubMed: 16313391]

Dodou E, et al. Mef2c is a direct transcriptional target of ISL1 and GATA factors in the anterior heart field during mouse embryonic development. Development 2004;131:3931–42. [PubMed: 15253934]

Edmondson DG, et al. Mef2 gene expression marks the cardiac and skeletal muscle lineages during mouse embryogenesis. Development 1994;120:1251–63. [PubMed: 8026334]

Ghanem N, et al. Regulatory roles of conserved intergenic domains in vertebrate Dlx bigene clusters. Genome Res 2003;13:533–43. [PubMed: 12670995]

Gregoire S, et al. Control of MEF2 transcriptional activity by coordinated phosphorylation and sumoylation. J Biol Chem 2006;281:4423–33. [PubMed: 16356933]

Gregoire S, Yang XJ. Association with class IIa histone deacetylases upregulates the sumoylation of MEF2 transcription factors. Mol Cell Biol 2005;25:2273–87. [PubMed: 15743823]

Han J, et al. Activation of the transcription factor MEF2C by the MAP kinase p38 in inflammation. Nature 1997;386:296–9. [PubMed: 9069290]

Ivey K, et al. Galphaq and Galpha11 proteins mediate endothelin-1 signaling in neural crest-derived pharyngeal arch mesenchyme. Dev Biol 2003;255:230–7. [PubMed: 12648486]

Jerome LA, Papaioannou VE. DiGeorge syndrome phenotype in mice mutant for the T-box gene, Tbx1. Nat Genet 2001;27:286–91. [PubMed: 11242110]

Kato Y, et al. Big mitogen-activated kinase regulates multiple members of the MEF2 protein family. J Biol Chem 2000;275:18534–40. [PubMed: 10849446]

Kelly PD, et al. Genetic linkage mapping of zebrafish genes and ESTs. Genome Res 2000;10:558–67. [PubMed: 10779498]

Kempf H, et al. Pharmacological inactivation of the endothelin type A receptor in the early chick embryo: a model of mispatterning of the branchial arch derivatives. Development 1998;125:4931–41. [PubMed: 9811577]

Kimmel CB, et al. Stages of embryonic development of the zebrafish. Dev Dyn 1995;203:253–310. [PubMed: 8589427]

Kimmel CB, et al. The shaping of pharyngeal cartilages during early development of the zebrafish. Dev Biol 1998;203:245–63. [PubMed: 9808777]

Kimmel CB, et al. Endothelin 1-mediated regulation of pharyngeal bone development in zebrafish. Development 2003;130:1339–51. [PubMed: 12588850]

Knapik EW, et al. A microsatellite genetic linkage map for zebrafish (Danio rerio). Nat Genet 1998;18:338–43. [PubMed: 9537415]

Kurihara Y, et al. Elevated blood pressure and craniofacial abnormalities in mice deficient in endothelin-1. Nature 1994;368:703–10. [PubMed: 8152482]

Lawson ND, Weinstein BM. In vivo imaging of embryonic vascular development using transgenic zebrafish. Dev Biol 2002;248:307–18. [PubMed: 12167406]

Lazaro JB, et al. Cyclin D-cdk4 activity modulates the subnuclear localization and interaction of MEF2 with SRC-family coactivators during skeletal muscle differentiation. Genes Dev 2002;16:1792–805. [PubMed: 12130539]

Lin CY, et al. Myogenic regulatory factors Myf5 and Myod function distinctly during craniofacial myogenesis of zebrafish. Dev Biol 2006;299:594–608. [PubMed: 17007832]

Lin Q, et al. Requirement of the MADS-box transcription factor MEF2C for vascular development. Development 1998;125:4565–74. [PubMed: 9778514]

Lin Q, et al. Control of mouse cardiac morphogenesis and myogenesis by transcription factor MEF2C. Science 1997;276:1404–7. [PubMed: 9162005]

Lindsay EA, et al. Tbx1 haploinsufficieny in the DiGeorge syndrome region causes aortic arch defects in mice. Nature 2001;410:97–101. [PubMed: 11242049]

Liu D, et al. Fgf3 and Fgf8 dependent and independent transcription factors are required for otic placode specification. Development 2003;130:2213–24. [PubMed: 12668634]

Lu J, et al. Signal-dependent activation of the MEF2 transcription factor by dissociation from histone deacetylases. Proc Natl Acad Sci U S A 2000;97:4070–5. [PubMed: 10737771]

Lyons GE, et al. Expression of mef2 genes in the mouse central nervous system suggests a role in neuronal maturation. J Neurosci 1995;15:5727–38. [PubMed: 7643214]

McKinsey TA, et al. Control of muscle development by dueling HATs and HDACs. Curr Opin Genet Dev 2001;11:497–504. [PubMed: 11532390]

Merscher S, et al. TBX1 is responsible for cardiovascular defects in velo-cardiofacial/DiGeorge syndrome. Cell 2001;104:619–29. [PubMed: 11239417]

Miller CT, Kimmel CB. Morpholino phenocopies of endothelin 1 (sucker) and other anterior arch class mutations. Genesis 2001;30:186–7. [PubMed: 11477704]

Miller CT, et al. moz regulates Hox expression and pharyngeal segmental identity in zebrafish. Development 2004;131:2443–61. [PubMed: 15128673]

Miller CT, et al. sucker encodes a zebrafish Endothelin-1 required for ventral pharyngeal arch development. Development 2000;127:3815–28. [PubMed: 10934026]

Miller CT, et al. Two endothelin 1 effectors, hand2 and bapx1, pattern ventral pharyngeal cartilage and the jaw joint. Development 2003;130:1353–65. [PubMed: 12588851]

Molkentin JD, et al. Mutational analysis of the DNA binding, dimerization, and transcriptional activation domains of MEF2C. Mol Cell Biol 1996a;16:2627–36. [PubMed: 8649370]

Molkentin JD, et al. Phosphorylation of the MADS-Box transcription factor MEF2C enhances its DNA binding activity. J Biol Chem 1996b;271:17199–204. [PubMed: 8663403]

Morasso MI, et al. Placental failure in mice lacking the homeobox gene Dlx3. Proc Natl Acad Sci U S A 1999;96:162–7. [PubMed: 9874789]

Nair S, et al. Requirements for Endothelin type-A receptors and Endothelin-1 signaling in the facial ectoderm for the patterning of skeletogenic neural crest cells in zebrafish. Development 2007;134:335–45. [PubMed: 17166927]

Neff MM, et al. dCAPS, a simple technique for the genetic analysis of single nucleotide polymorphisms: experimental applications in Arabidopsis thaliana genetics. Plant J 1998;14:387–92. [PubMed: 9628033]

Neuhauss SC, et al. Mutations affecting craniofacial development in zebrafish. Development 1996;123:357–67. [PubMed: 9007255]

Nissen RM, et al. Zebrafish foxi one modulates cellular responses to Fgf signaling required for the integrity of ear and jaw patterning. Development 2003;130:2543–54. [PubMed: 12702667]

Ozeki H, et al. Endothelin-1 regulates the dorsoventral branchial arch patterning in mice. Mech Dev 2004;121:387–95. [PubMed: 15110048]

Park BK, et al. Intergenic enhancers with distinct activities regulate Dlx gene expression in the mesenchyme of the branchial arches. Dev Biol 2004;268:532–45. [PubMed: 15063187]

Piotrowski T, et al. The zebrafish van gogh mutation disrupts tbx1, which is involved in the DiGeorge deletion syndrome in humans. Development 2003;130:5043–52. [PubMed: 12952905]

Piotrowski T, et al. Jaw and branchial arch mutants in zebrafish II: anterior arches and cartilage differentiation. Development 1996;123:345–56. [PubMed: 9007254]

Qiu M, et al. Null mutation of Dlx-2 results in abnormal morphogenesis of proximal first and second branchial arch derivatives and abnormal differentiation in the forebrain. Genes Dev 1995;9:2523–38. [PubMed: 7590232]

Ruest LB, et al. Endothelin-A receptor-dependent and -independent signaling pathways in establishing mandibular identity. Development 2004;131:4413–23. [PubMed: 15306564]

Schilling TF, Kimmel CB. Musculoskeletal patterning in the pharyngeal segments of the zebrafish embryo. Development 1997;124:2945–60. [PubMed: 9247337]

Schilling TF, et al. Jaw and branchial arch mutants in zebrafish I: branchial arches. Development 1996;123:329–44. [PubMed: 9007253]

Schulte-Merker S, et al. Expression of zebrafish goosecoid and no tail gene products in wild-type and mutant no tail embryos. Development 1994;120:843–52. [PubMed: 7600961]

Sumiyama K, et al. The role of gene duplication in the evolution and function of the vertebrate Dlx/distal-less bigene clusters. J Struct Funct Genomics 2003;3:151–9. [PubMed: 12836694]

Thomas T, et al. A signaling cascade involving endothelin-1, dHAND and msx1 regulates development of neural-crest-derived branchial arch mesenchyme. Development 1998;125:3005–14. [PubMed: 9671575]

Ticho BS, et al. Three zebrafish MEF2 genes delineate somitic and cardiac muscle development in wild-type and mutant embryos. Mech Dev 1996;59:205–18. [PubMed: 8951797]

Walker MB, et al. Zebrafish furin mutants reveal intricacies in regulating Endothelin1 signaling in craniofacial patterning. Dev Biol 2006a;295:194–205. [PubMed: 16678149]

Walker MB, et al. phospholipase C, beta 3 is required for Endothelin1 regulation of pharyngeal arch patterning in zebrafish. Dev Biol. 2006b

Walker MB, Kimmel CB. A two-color acid-free cartilage and bone stain for zebrafish larvae. Biotech. Histochem 82in press

Westerfield, M. The Zebrafish book : a guide for the laboratory use of zebrafish (Brachydanio rerio). University of Oregon Press; Eugene. Or.: 1993.

Xu D, et al. ECE-1: a membrane-bound metalloprotease that catalyzes the proteolytic activation of big endothelin-1. Cell 1994;78:473–85. [PubMed: 8062389]

Yanagisawa H, et al. Targeted deletion of a branchial arch-specific enhancer reveals a role of dHAND in craniofacial development. Development 2003;130:1069–78. [PubMed: 12571099]

Yanagisawa H, et al. Dual genetic pathways of endothelin-mediated intercellular signaling revealed by targeted disruption of endothelin converting enzyme-1 gene. Development 1998;125:825–36. [PubMed: 9449665]

Zang MX, et al. Cooperative activation of atrial naturetic peptide promoter by dHAND and MEF2C. J Cell Biochem 2004;93:1255–66. [PubMed: 15486975]

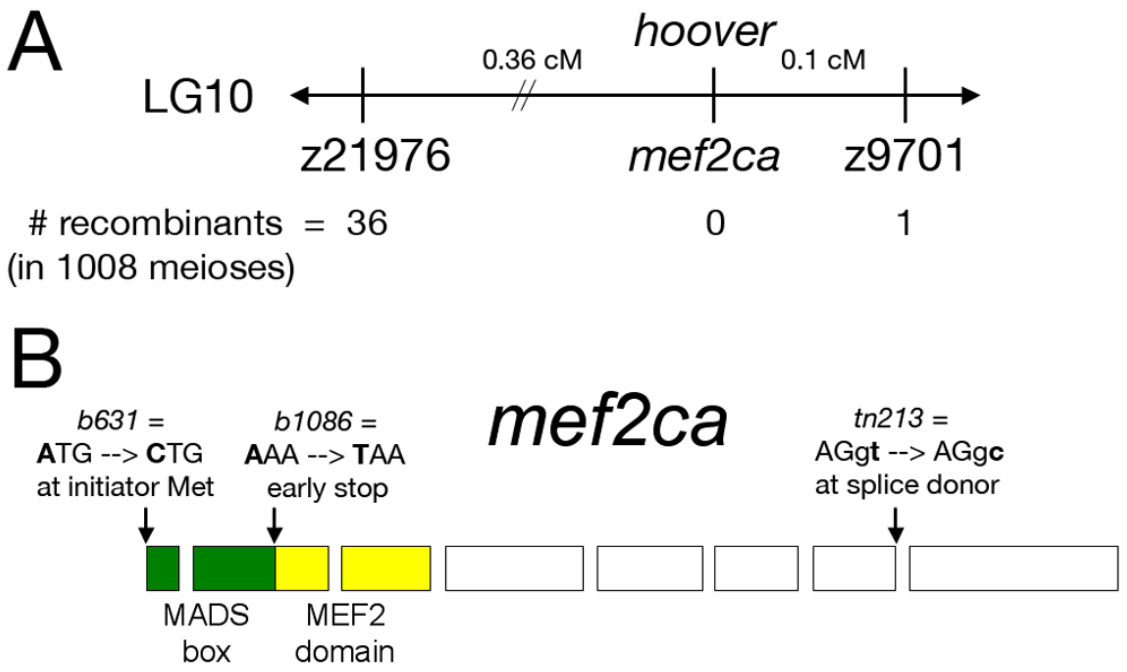

Fig. 1.

Molecular identification of the lesions in *hoover(mef2ca)* mutants. (A) Schematic showing the map position of *hoover*, which is non-recombinant with *mef2ca* in 1008 meioses. (B) *mef2ca* is mutated in all three *hoover* alleles. In *b631* mutants, an A-to-C mutation is predicted to change the initiator methionine to leucine. In *b1086* mutants, an A-to-T mutation creates an early stop in exon two, predicted to create a truncated protein lacking a MEF2 domain. In *tn213* mutants, a T-to-C mutation alters the conserved second nucleotide of the intron 7 splice donor.

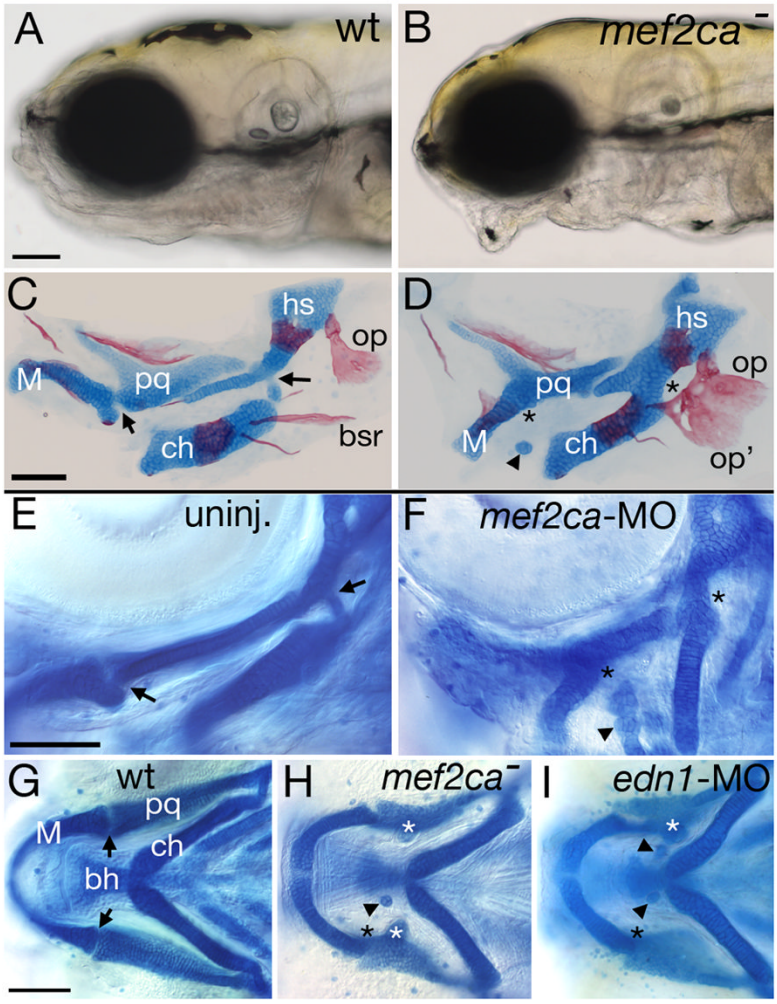

Fig. 2.

Reduction of *mef2ca* function causes facial deformities which phenocopy partial *edn1* loss-of-function. (A-B) Live phenotypes of *mef2ca* mutants at 5 dpf. *mef2ca* mutants have malformed faces, open mouths, and ventrally displaced jaws. (C-D) Cartilage and bone phenotypes in the pharyngeal arches of *mef2ca* mutants. Dorsal/ventral joints (arrows) are missing in *mef2ca* mutants (asterisks). Mutants also have ectopic cartilage nodules (arrowhead), distinctive ectopic medial processes emanating from the upper jaw cartilage (see Table 2) and homeotic transformations of hyoid dermal bone identity. In *mef2ca* mutants, a ventral hyoid bone, the branchiostegal ray, is enlarged, assumes the shape of and fuses to the dorsal hyoid bone, the opercle. (E-F) mef2ca-MO injection phenocopies *mef2ca* mutations. Lateral views of wholemount 4.5 dpf wild-type larvae, uninjected (E) and injected with 5 ng of *mef2ca* morpholino (F). mef2ca-MO injected fish display characteristic *mef2ca* mutant cartilage phenotypes. Joints are lost (asterisks) and ectopic cartilage nodules (arrowhead) are seen near the basihyal. (G-I) *mef2ca* mutation phenocopies gradual reduction in *edn1* function. Ventral views of 4.5 dpf Alcian stained wild-type (G), *mef2ca*^{b631} mutant (H), and low level edn1-MO injected (I) larvae. *mef2ca* mutants and low level edn1-MO morphants display joint loss (black asterisks), ectopic medially-projecting processes on the upper jaw cartilage, the palatoquadrate (white asterisks), and ectopic cartilage nodules near the basihyal (arrowheads). bh, basihyal; bsr, branchiostegal ray; ch, ceratohyal; hs, hyosymplectic; M, Meckel's; op, opercle; pq, palatoquadrate.

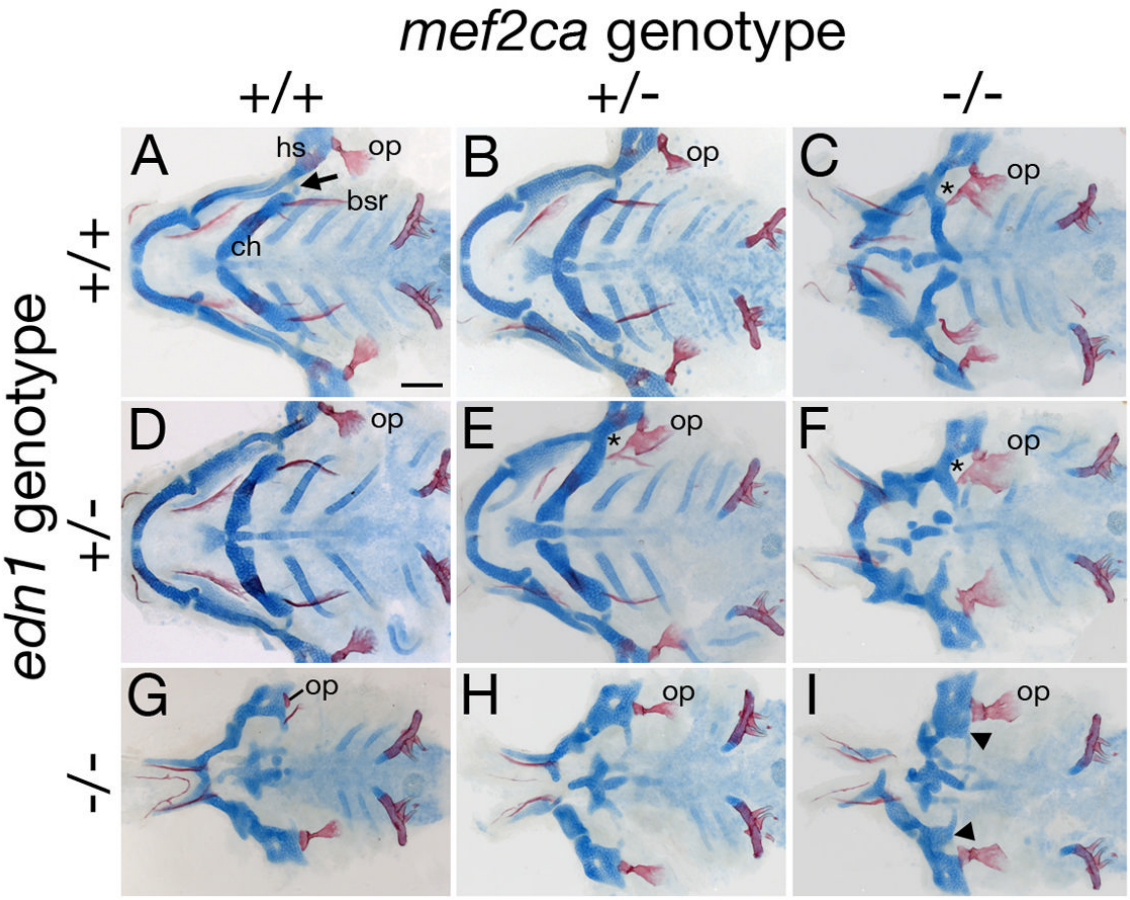

Fig. 3.

Complex genetic interactions between *mef2ca* and *edn1*. Flat-mounted pharyngeal skeletons of 5 dpf fish stained for cartilage in blue and bone in red for fish of different *mef2ca* and *edn1* genotypes. (A) In the wild-type second arch, a prominent fan-shaped opercle bone (op) articulates with the hyosymplectic (hs). Its serial homolog, the branchiostegal ray (bsr) appears saber-shaped and articulates with the ceratohyal (ch). We typically detect no phenotypes in *edn1* or *mef2ca* single heterozygous classes (B and D), although rarely very mild phenotypes are seen in *edn1* mutant heterozygotes (Table 2). (C) In *mef2ca* homozygous mutants, the opercle is enlarged, and the ventral branchiostegal ray is enlarged and transformed towards opercle morphology. The dorsal/ventral joint is lost (asterisk showing joint loss in the hyoid arch). The hyoid ventral cartilage is reduced. (E) Fish heterozygous for both *mef2ca* and *edn1* (*mef2ca*+/−; *edn1*+/−) display *mef2ca* mutant phenotypes such as joint loss (asterisk) and enlarged opercles fused to malformed branchiostegal rays. (F) Heterozygosity of *edn1* enhances the *mef2ca* cartilage and bone phenotypes (compare to C, and see Table 2). (G-I) Heterozygosity for *mef2ca* mutation (H) partially and subtly rescues cartilage and bone phenotypes in *edn1*−/− homozygous mutants (G), while homozygosity for *mef2ca* mutation more significantly partially rescues hyoid cartilage and bone phenotypes of *edn1* homozygous mutants (I).

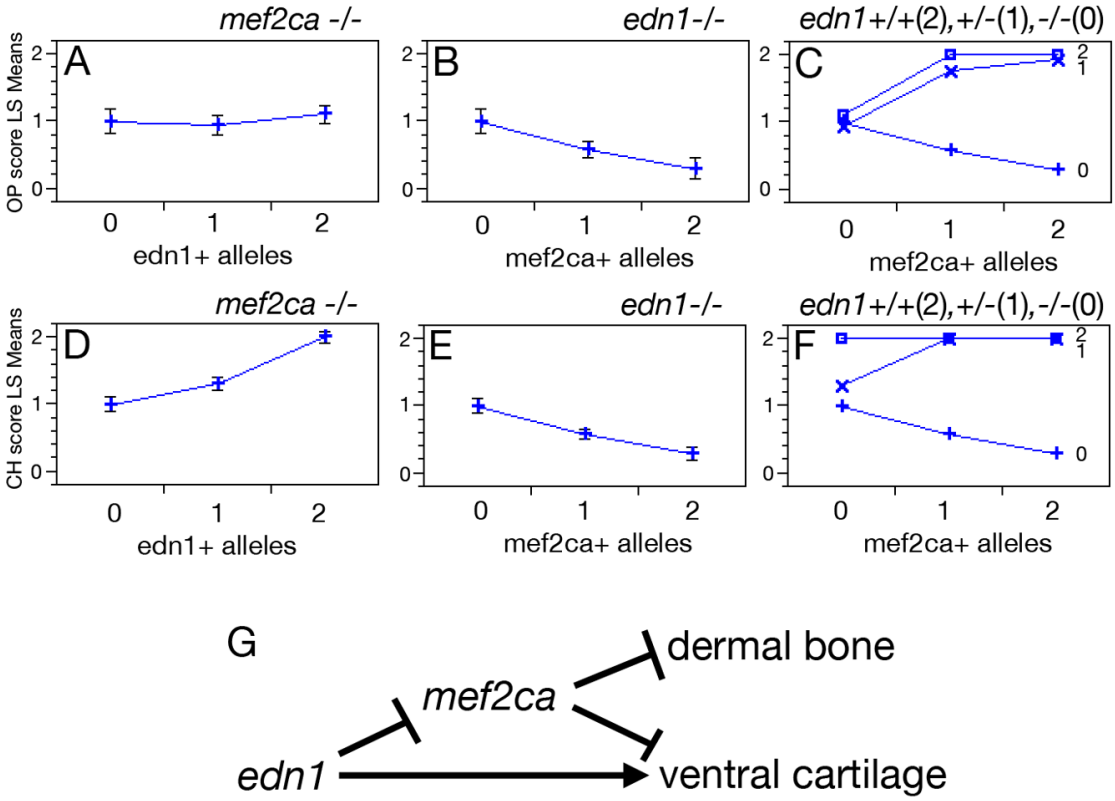

Fig. 4.

Epistatic interactions between *mef2ca* and *edn1*. Hyoid bone (opercle, OP) (A-C) and cartilage (ceratohyal, CH) (D-F) phenotypes as a function of: *edn1*+ alleles in homozygous *mef2ca* mutants (A,D), *mef2ca*+ alleles in homozygous *edn1* mutants (B, E), and genotypes at both *mef2ca* and *edn1* (C,F). In C and F, *edn1* genotype is denoted by the number of *edn1*+ alleles: open box = 2 *edn1*+ alleles; "X" = 1 *edn1*+ allele, "+" = 0 *edn1*+ alleles. Phenotypes were scored on individual sides of PCR-genotyped larvae (see Methods). OP bone scoring scale: strong *edn1* loss-of-function phenotype (loss of bone) = 0, weak *edn1* loss-of-function phenotype (expanded bone) = 1, wild-type = 2. CH cartilage scoring scale: strong *edn1* loss-of-function phenotype (complete loss) = 0, weak *edn1* loss-of-function phenotype (partial loss) = 1, wild-type = 2. See Kimmel et al. (2003) and Miller and Kimmel (2001) for strong and weak *edn1* loss-of-function bone and cartilage mutant phenotypes. Phenotypes for each genotypic category are shown as least square means (LS means). Error bars represent 95% confidence intervals from ANOVA. (G) Genetic model for zebrafish hyoid cartilage and dermal bone development. *mef2ca* represses bone and cartilage formation. *edn1* represses *mef2ca*, but also activates a *mef2ca*-independent pathway for ventral cartilage development.

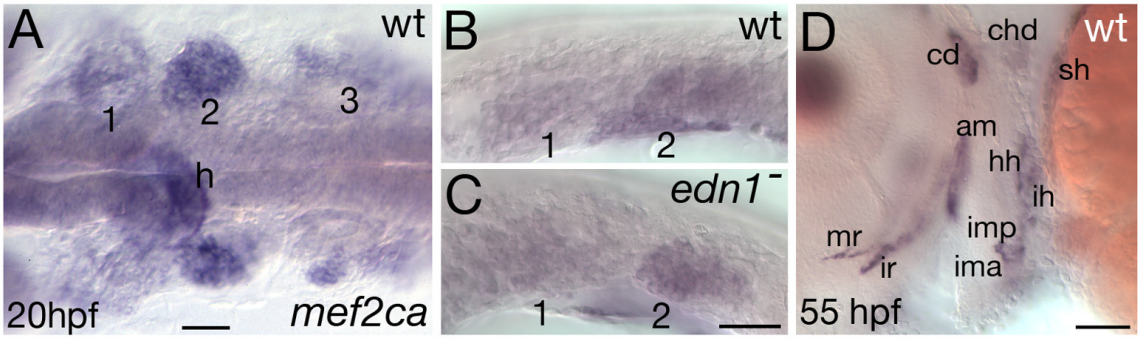

Fig. 5.

mef2ca expression in early CNC and late head muscles. In situ hybridization showing *mef2ca* expression in wild-type (A,B,D) and *edn1* mutant (C) embryos at 20 hpf (A-C) and 55 hpf (D). (A-B) Dorsal (A) and lateral (B) views of *mef2ca* expression in all three migrating streams of CNC at 20 hpf. (C) CNC expression in *edn1* mutants appears unaffected. (D) Lateral view of *mef2ca* expression in head muscles at 55 hpf. For A-C, arches are numbered. Pharyngeal pouches are outlined in B-C. For description of the larval head muscle pattern see (Lin et al., 2006; Schilling and Kimmel, 1997). am adductor mandibulae; cd, constrictor dorsalis; chd, constrictor hyoideus dorsalis; hh, hyohyoideus; ih, interhyoideus; ima, intermandibularis anterior; imp, intermandibularis posterior; ir, inferior rectus; mr, medial rectus; sh, sternohyoideus.

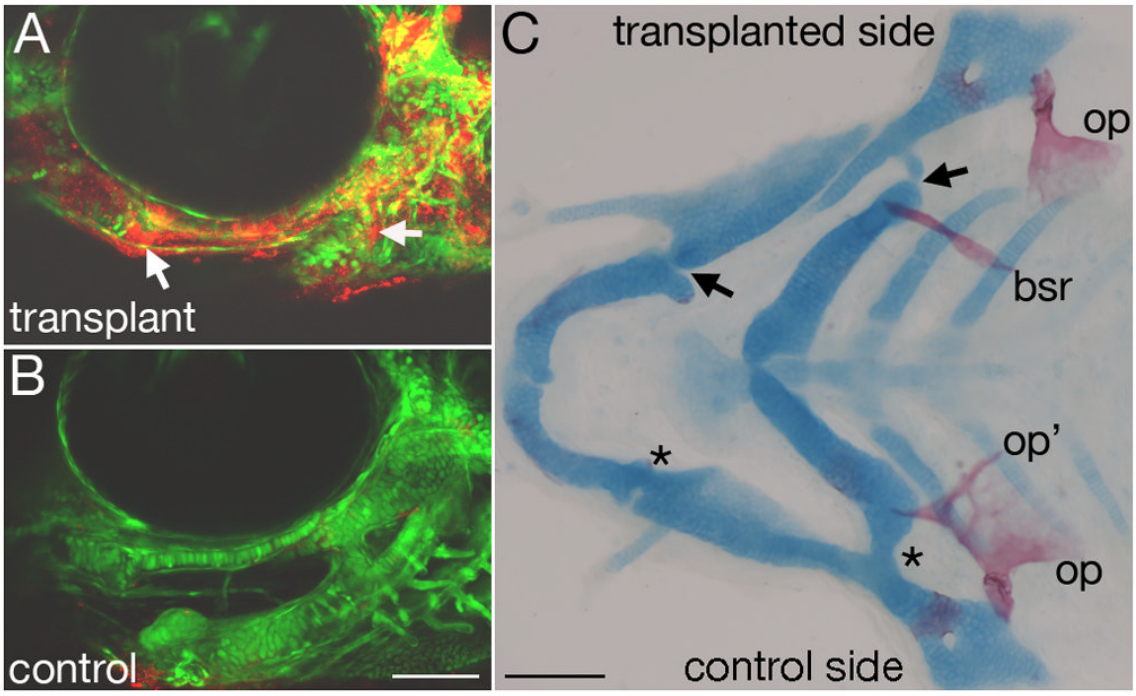

Fig. 6.

mef2ca is autonomously required in cranial neural crest for skeletal patterning. Wild-type rhodamine-labeled *fli1:EGFP* CNC cells were unilaterally transplanted into *mef2ca* mutant hosts. (A-B) Confocal micrographs of *mef2ca* mutant with wild-type CNC mosaic fish from the tranplanted side (A) and control side (B). On the transplanted side, lineage tracer is detected throughout dorsal and ventral cartilages, as well as joint regions (arrows). On the control side, only *mef2ca* mutant host *fli1:GFP* CNC derivatives are seen. (C) Flatmounted pharyngeal skeleton, double stained for cartilage in blue and bone in red. Dorsal/ventral cartilage joints have been rescued on the transplanted side (arrows) but not on the control side (asterisks). Opercle and branchiostegal ray morphology is also completely rescued on the transplanted side, but not the control side. bsr, branchiostegal ray; op, opercle.

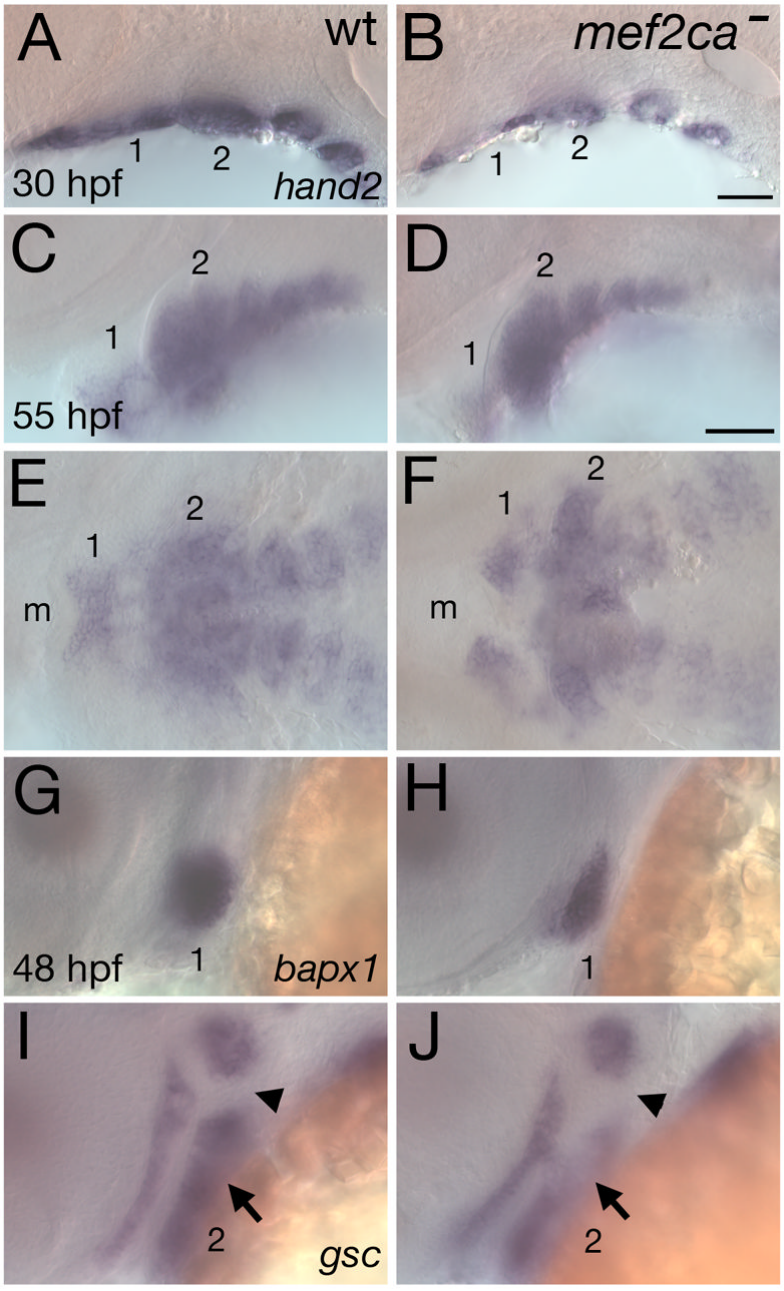

Fig. 7.

mef2ca is required for proper expression of *hand2*, *bapx1*, and *gsc* in postmigratory CNC. Lateral (A-D, G-J) and ventral (E,F) views of expression of *hand2* (A-F) at 30 hpf (A,B) and 55 hpf (C-F), and *bapx1* (G,H) and *gsc* (I,J) at 48 hpf in wild-type (A,C,E,G,I) and *mef2ca* mutants (B,D,F,H,J). (A-F) Ventrally restricted expression of *hand2* is reduced in *mef2ca* mutants at 30 hpf, but recovers by 55 hpf. (G,H) *bapx1* expression prefiguring the jaw joint is reduced in *mef2ca* mutants. (I,J) Ventral hyoid expression of *gsc* (arrow) is downregulated in *mef2ca* mutants. The hyoid joint region (arrowhead) remains devoid of *gsc* expression. Arches are numbered. m, mouth.

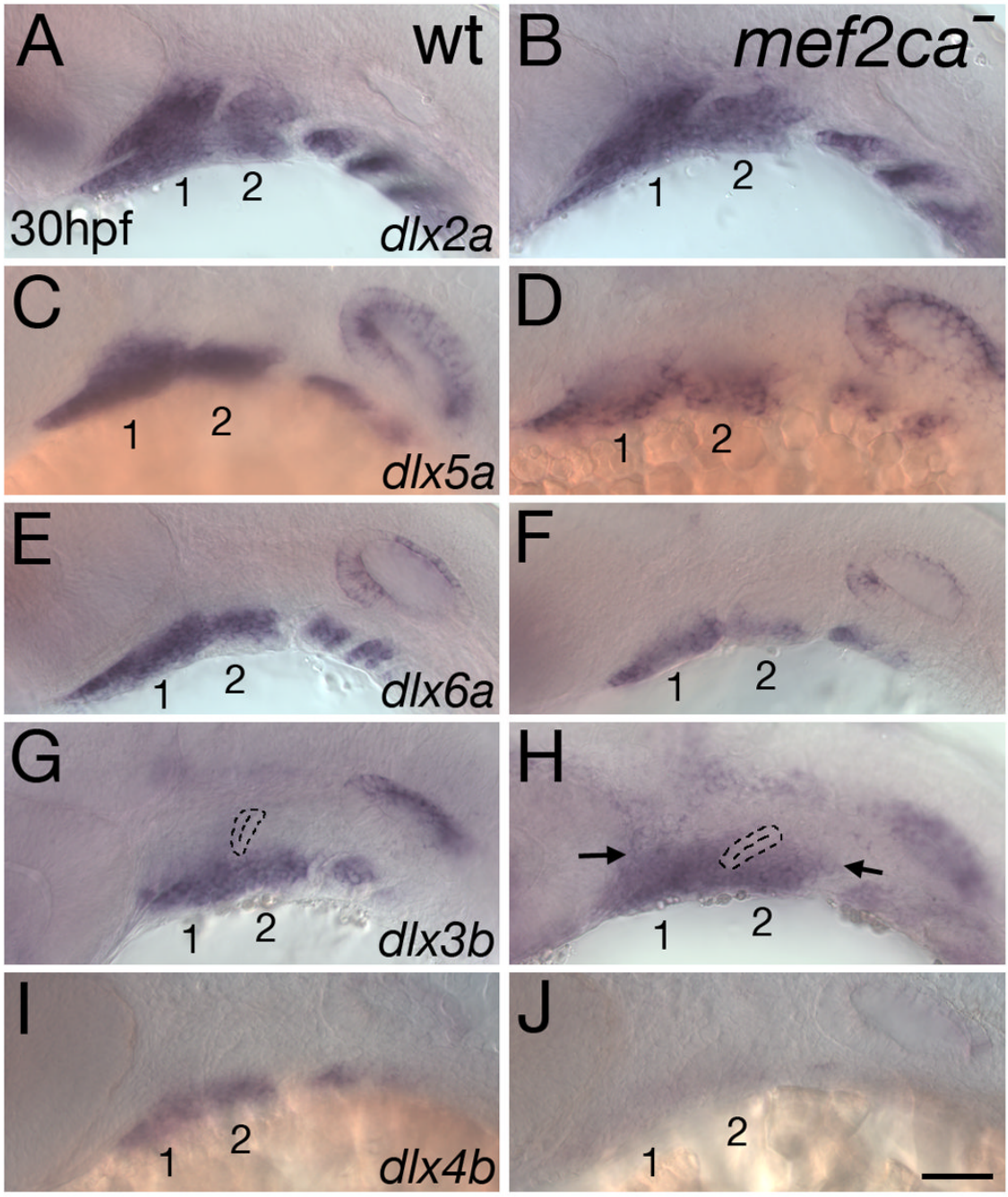

Fig. 8.

mef2ca activates *dlx5a*, *dlx6a*, and *dlx4b* but represses *dlx3b*. Lateral views of expression of *dlx2a* (A,B), *dlx5a* (C,D), *dlx6a* (E,F), *dlx3b* (G,H) and *dlx4b* (I,J) in wild-type (A,C,E,G,I) and *mef2ca* mutant (B,D,F,H,J) heads of 30 hpf zebrafish embryos. (A,B) *mef2ca* mutants have no detectable alteration in *dlx2a* expression, which is expressed throughout pharyngeal arch CNC. (C-F) Expression of both *dlx5a* and *dlx6a*, in ventral and intermediate CNC in wild-types, is reduced in *mef2ca* mutants. (G,H) *dlx3b* expression is ectopically expressed in dorsal arch CNC of *mef2ca* mutants (arrows). (I,J) In contrast, *dlx4b* expression, restricted to ventral arch CNC, is largely undetectable in *mef2ca* mutants. The first two arches are numbered.

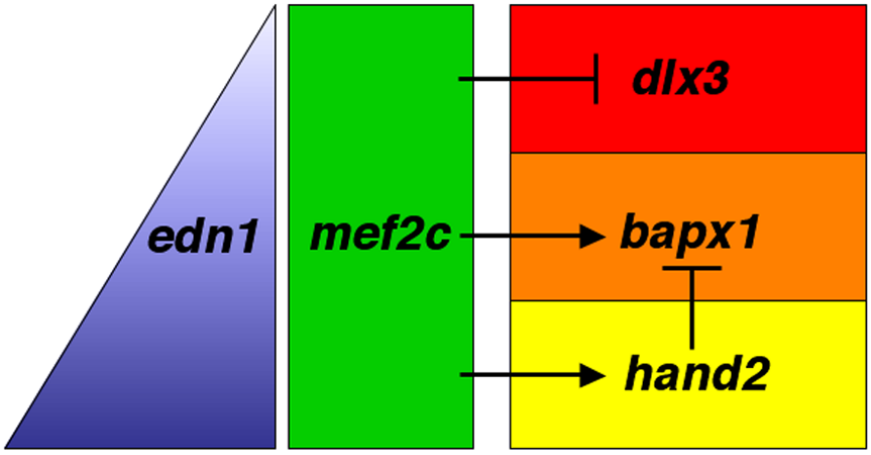

Fig. 9.

The *edn1*-effector *mef2c* regulates dorsal/ventral patterning in pharyngeal arch CNC. Edn1 secreted from ventral pharyngeal epithelia and mesoderm forms a gradient of Edn1 (blue triangle), with high levels ventrally (bottom of triangle) and low levels dorsally (top of triangle). *mef2c*, broadly expressed in early arch postmigratory CNC (green rectangle) exerts differential effects on downstream target genes to help specify domains along the dorsal-ventral axis. In the dorsal arch (red), *mef2c* represses *dlx3* expression. In the intermediate (orange) and ventral (yellow) domains, *mef2c* activates transcription of *bapx1* and *hand2*, two effectors of intermediate and ventral skeletal fates, respectively. *hand2* helps delimit the intermediate domain by repressing *bapx1* expression from the ventral domain (Miller et al., 2003). The red, orange, and yellow domains are in part defined by the nested expression patterns of *dlx* genes and *hand2*. The dorsal red domain expresses *dlx2a*, but not *dlx3b* or *dlx6a*. The orange and yellow domains express *dlx2a*, *dlx3b*, *dlx5a*, and *dlx6a*. The expression of *hand2* defines the ventral yellow compartment. See Walker et al. (2006a) for a more detailed spatiotemporal model of *dlx* and *hand2* regulation by Edn1.

Table 1

mef2ca mutant phenotypes resemble partial loss of *edn1* function phenotypes

		% with Joint Loss in:							
		arch 1			arch 2				
			unilateral			unilateral			
allele	n	bilateral	Left	Right	bilateral	Left	Right	% with BHN	% with PQP
b1086	64	97	0	2	95	0	3	52	77
tn213	63	87	6	6	70	9	8	78	30
b631	365	38	7	28	5	1	3	26	73
mef2ca-MO:									
5 ng	135	81	6	6	47	5	7	55	15
1.5 ng	29	0	14	17	0	0	0	7	0
edn1-MO									
0.5 ng	105*	23	3	7	32	4	10	21	21

Pharyngeal cartilage phenotypes seen in 4.5 dpf larvae for all three alleles of *mef2ca*, *mef2ca* morphants, and low-level *edn1* morphants. Joint loss refers to absence of a joint between dorsal and ventral pharyngeal cartilages. BHN, ectopic nubbin of cartilage around basihyal; PQP, ectopic medial process emanating from palatoquadrate (see Fig. 2G-I).

*Of 242 fish injected with 0.5 ng edn1-MO, 119 had no detectable cartilage phenotype and 18 had very severe phenotypes resembling *edn1* mutant larvae. The percentages listed here are of the 105 larvae with phenotypes weaker than the *edn1* mutant phenotype.